

AN OVERLAPPING SCHWARZ ALGORITHM FOR ALMOST INCOMPRESSIBLE ELASTICITY

CLARK R. DOHRMANN* AND OLOF B. WIDLUND †

Abstract. Overlapping Schwarz methods are extended to mixed finite element approximations of linear elasticity which use discontinuous pressure spaces. The coarse component of the preconditioner is based on a low-dimensional space previously developed for scalar elliptic problems and a domain decomposition method of iterative substructuring type, i.e., a method based on non-overlapping decompositions of the domain, while the local components of the preconditioner are based on solvers on a set of overlapping subdomains. A bound is established for the condition number of the algorithm which grows in proportion to the square of the logarithm of the number of degrees of freedom in individual subdomains and the third power of the relative overlap between the overlapping subdomains, and which is independent of the Poisson ratio as well as jumps in the Lamé parameters across the interface between the subdomains. A positive definite reformulation of the discrete problem makes the use of the standard preconditioned conjugate gradient method straightforward. Numerical results, which include a comparison with problems of compressible elasticity, illustrate the findings.

Key words. domain decomposition, overlapping Schwarz, preconditioners, iterative methods, almost incompressible elasticity, mixed finite element methods

AMS subject classifications. 65F10, 65N30, 65N55

1. Introduction. The subject of this paper is an overlapping Schwarz algorithm for almost incompressible elasticity problems. Previous theory for overlapping Schwarz methods has been restricted to compressible cases in which the Poisson ratio ν is bounded away from its maximum possible value of $1/2$; see [33, Section 8]. Here, we remove this restriction, and present a coarse space which effectively accommodates all positive values of $\nu < 1/2$. This coarse space is an extension of a component of an iterative substructuring method developed over a decade ago for scalar elliptic problems; see [17] and also [33, Algorithm 5.16]. Recent applications of such extended coarse spaces to a variety of different problem types appear in [14]. We note that the coarse space presented here has already been used successfully as part of a production-level iterative solver in the parallel structural dynamics code Salinas [4].

An early application of overlapping Schwarz methods to mixed formulations of linear elasticity and Stokes problems is given in [22]. In that work, the coarse spaces were based on the same mixed finite element methods on coarse meshes and both continuous and discontinuous pressure spaces were considered. An analysis of these methods was not provided, but their performance was shown to be quite competitive with block diagonal and block triangular preconditioners, see [23].

Related iterative substructuring approaches for either incompressible or almost incompressible problems appear in [13, 19, 27, 28]. For each of these methods, special care is required to ensure that the coarse space is properly constructed. As a result, standard coarse spaces for compressible problems must be modified and enriched to accommodate incompressible or almost incompressible cases. The coarse space

*Sandia National Laboratories, Albuquerque, NM 87185, USA crdohrm@sandia.gov Sandia is a multiprogram laboratory operated by Sandia Corporation, a Lockheed Martin Company, for the United States Department of Energy's National Nuclear Security Administration under contract DE-AC04-94AL85000.

†Courant Institute, 251 Mercer Street, New York NY 10012, USA widlund@cims.nyu.edu This work was supported in part by the U.S. Department of Energy under contracts DE-FG02-06ER25718 and DE-FC02-01ER25482 and in part by National Science Foundation Grant DMS-0513251.

presented in this paper can be applied without modification to both compressible and almost incompressible cases. In addition, our approach does not require access to individual subdomain matrices, i.e., we can work directly with a globally assembled matrix.

We restrict attention in the present work to finite elements with discontinuous pressure interpolation. By doing so, it is possible to eliminate the pressure unknowns at the element level. An important consequence is that the same algorithm, as for compressible elasticity, can be used for almost incompressible cases, since the assembled matrix is symmetric and positive definite, and the method of preconditioned conjugate gradients can be used as the iterative method.

In addition to almost incompressible elasticity, we hope that our work will have an impact on the development of penalty-based and augmented Lagrangian preconditioners for saddle point systems as in [2, 3, 11, 16]. In particular, the present work would be relevant to the practical implementation of such preconditioners for incompressible Stokes and Navier Stokes equations. This is the case because the algorithm presented here effectively handles the case of ν approaching $1/2$, i.e., the incompressible limit.

An overview of mixed finite elements for elasticity is given in Section 2. Section 3 is devoted to the development of Lemma 3.3, which is central to the proof of our main result. This lemma, and properties of the chosen coarse space, allow us to apply some existing theory for compressible problems to almost incompressible cases. The proof of our main result, a condition number bound for the algorithm, is provided in Section 5. In Section 6, we consider the extension of our results to subdomains with boundaries which are not very regular, basing the discussion on our recent work [15, 25]. The paper concludes with supporting numerical examples and a discussion in Section 7.

2. Almost incompressible elasticity and mixed finite elements. Let $\Omega \subset \mathbb{R}^n$, $n = 2, 3$, be a domain and let $\partial\Omega_D$ be a nonempty subset of its boundary $\partial\Omega$ and introduce the Sobolev space $\mathbf{V} := \{\mathbf{v} \in \mathbf{H}^1(\Omega) : \mathbf{v}|_{\partial\Omega_D} = 0\}$. Here $\mathbf{H}^1(\Omega) := H^1(\Omega)^n$. The linear elasticity problem consists in finding the displacement $\mathbf{u} \in \mathbf{V}$ of the domain Ω , fixed along $\partial\Omega_D$, and subject to a surface force of density \mathbf{g} , along $\partial\Omega_N = \partial\Omega \setminus \partial\Omega_D$, and a body force \mathbf{f} :

$$2 \int_{\Omega} \mu \epsilon(\mathbf{u}) : \epsilon(\mathbf{v}) \, dx + \int_{\Omega} \lambda \operatorname{div} \mathbf{u} \operatorname{div} \mathbf{v} \, dx = \langle \mathbf{F}, \mathbf{v} \rangle \quad \forall \mathbf{v} \in \mathbf{V}. \quad (2.1)$$

Here $\lambda(x)$ and $\mu(x)$ are the Lamé parameters, $\epsilon_{ij}(\mathbf{u}) = \frac{1}{2}(\frac{\partial u_i}{\partial x_j} + \frac{\partial u_j}{\partial x_i})$ the linearized strain tensor, and the inner products are defined by

$$\epsilon(\mathbf{u}) : \epsilon(\mathbf{v}) = \sum_{i=1}^n \sum_{j=1}^n \epsilon_{ij}(\mathbf{u}) \epsilon_{ij}(\mathbf{v}), \quad \langle \mathbf{F}, \mathbf{v} \rangle = \int_{\Omega} \sum_{i=1}^n f_i v_i \, dx + \int_{\partial\Omega_N} \sum_{i=1}^n g_i v_i \, dA.$$

The Lamé parameters can be expressed in terms of the Poisson ratio ν and Young's modulus E :

$$\lambda = \frac{E\nu}{(1+\nu)(1-2\nu)}, \quad \mu = \frac{E}{2(1+\nu)}.$$

The domain Ω is partitioned into non-overlapping subdomains Ω_i . In Section 6, we will discuss the regularity required of their boundaries for our arguments to be valid. We assume, for simplicity, that the Lamé parameters are constant in each

subdomain. Since much of our analysis will be carried out for one subdomain at a time, we can then work with problems with constant coefficients. The bound for the condition number of our algorithm will be independent of the values of all these parameters.

2.1. A saddle point formulation. When the material becomes almost incompressible, the Poisson ratio ν approaches the value $1/2$ and $\lambda/\mu = 2\nu/(1 - 2\nu)$ approaches infinity. In such cases, finite element discretizations of this pure displacement formulation will increasingly suffer from locking and very slow convergence of the finite element solution.

A well-known remedy is based on introducing the new variable $p = -\lambda \operatorname{div} \mathbf{u} \in U \subset L^2(\Omega)$, that we will call pressure, and replacing the pure displacement problem (2.1) with a mixed formulation: find $(\mathbf{u}, p) \in \mathbf{V} \times U$ such that

$$\left\{ \begin{array}{l} 2 \int_{\Omega} \mu \epsilon(\mathbf{u}) : \epsilon(\mathbf{v}) \, dx - \int_{\Omega} \operatorname{div} \mathbf{v} \, p \, dx = \langle \mathbf{F}, \mathbf{v} \rangle \quad \forall \mathbf{v} \in \mathbf{V} \\ - \int_{\Omega} \operatorname{div} \mathbf{u} \, q \, dx - \int_{\Omega} 1/\lambda \, pq \, dx = 0 \quad \forall q \in U; \end{array} \right. \quad (2.2)$$

see Brezzi and Fortin [8] or Brenner and Scott [7].

In the case of homogeneous Dirichlet boundary conditions for \mathbf{u} on all of $\partial\Omega$, we will choose $U := L_0^2(\Omega) := \{q \in L^2(\Omega) : \int_{\Omega} q \, dx = 0\}$, since it follows from the divergence theorem that the pressure will have a zero mean value. For nonzero Dirichlet boundary data, the same is true if the net flux satisfies $\int_{\partial\Omega} \mathbf{u} \cdot \mathbf{n} \, ds = 0$, where \mathbf{n} is the outward normal. If, on the other hand, the boundary conditions are mixed (part essential and part natural), then there is always a unique solution with a pressure component in $U = L^2(\Omega)$. Rather than discussing two somewhat different cases, we will, from now on, focus on the case with homogeneous Dirichlet boundary conditions on all of $\partial\Omega$.

The net fluxes $\int_{\partial\tilde{\Omega}} \mathbf{u} \cdot \mathbf{n} \, dA$, across the boundary $\partial\tilde{\Omega}$, of subsets $\tilde{\Omega}$ of individual subdomains will be important in our analysis. Only if they vanish, are there divergence-free extensions of the boundary values for which the bilinear form $\int_{\tilde{\Omega}} \lambda \operatorname{div} \mathbf{u} \operatorname{div} \mathbf{v} \, dx$ will then vanish.

In our analysis, we will work only with the restrictions of the equations (2.2) to individual subdomains Ω_i , or subsets of such subdomains. In such cases, we can factor out the constants μ and $1/\lambda$ and we will use the notation $a_i(\mathbf{u}, \mathbf{v})$, $b_i(\mathbf{v}, p)$, and $c_i(p, q)$ for the three resulting bilinear forms associated with the subdomain Ω_i .

We note that

$$(\operatorname{div} \mathbf{v}, \operatorname{div} \mathbf{v})_{L^2(\Omega_i)} \leq n \int_{\Omega_i} \epsilon(\mathbf{v}) : \epsilon(\mathbf{v}) \, dx = n/2 \, a_i(\mathbf{v}, \mathbf{v}), \quad n = 2, 3.$$

Therefore,

$$|b_i(\mathbf{v}, p)| = \left| - \int_{\Omega_i} \operatorname{div} \mathbf{v} \, p \, dx \right| \leq \sqrt{n/2} a_i(\mathbf{v}, \mathbf{v})^{1/2} c_i(p, p)^{1/2}. \quad (2.3)$$

In the absence of essential boundary conditions, the elasticity operator has zero energy modes, which are the rigid body modes. There are three of them for $n = 2$ and six for $n = 3$; see further Section 4.

By letting $\lambda/\mu \rightarrow \infty$, we obtain the limiting problem for incompressible linear elasticity and also a formulation of the Stokes system for incompressible fluids. A penalty term, as in the compressible case, could also originate from stabilization techniques or penalty formulations for Stokes problems.

A Korn inequality for the subspace orthogonal to the rigid body modes will establish an equivalence between the square of the norm in $\mathbf{H}^1(\Omega)$ and the bilinear form $a(\cdot, \cdot)$; see further Section 5. This will make it possible to use many tools and results developed in studies of scalar elliptic problems.

2.2. Finite element methods with discontinuous pressures. We assume that the domain Ω is decomposed into N non-overlapping subdomains Ω_i of diameter H_i . The interface of this decomposition is given by

$$\Gamma = \left(\bigcup_{i=1}^N \partial\Omega_i \right) \setminus \partial\Omega.$$

To simplify our discussion, we will assume, as in [33, Assumption 4.3], that each subdomain is the union of shape-regular triangular or tetrahedral elements of a global conforming coarse mesh and that the number of such triangles or tetrahedra forming any individual subdomain is uniformly bounded. In Section 6, we will explore the extent by which this assumption can be relaxed. Each subdomain is further partitioned into many shape-regular elements. We will assume that the nodes match across the interface between the subdomains.

In our experimental work, we have chosen to work with the $Q_2(h) - P_1(h)$ finite elements: the displacement space is $\mathbf{V}^h := (Q_2(h))^n$, while the pressure space consists of discontinuous, piecewise linear functions:

$$U^h := \{q \in U : q|_T \in P_1(T) \quad \forall T \in \tau_h\}.$$

The two spaces are defined on the same quadrilateral or hexahedral mesh. This mixed finite element method satisfies a uniform inf-sup condition:

$$\sup_{\mathbf{v} \in \mathbf{V}^h} \frac{b_i(\mathbf{v}, q)}{a_i(\mathbf{v}, \mathbf{v})^{1/2}} \geq \beta c_i(q, q)^{1/2} \quad \forall q \in U^h \cap L_0^2, \quad \beta > 0. \quad (2.4)$$

The parameter β depends on the domain and, in particular, it varies inversely with the aspect ratio of the domain; see Section 5. There are optimal $O(h^2)$ error estimates for both displacements and pressures for this mixed finite element method; see Brezzi and Fortin [8, chap. VI, p. 216].

We note that while finite element methods based on hexahedra and quadrilaterals enjoy popularity, our theory applies equally well to any stable mixed method, e.g., one based on tetrahedra or triangles as long as the pressure space is discontinuous. We could also consider some more general saddle point problems with penalty terms.

3. Analysis of saddle point problems. Consider the linear system

$$\begin{bmatrix} \mu A & B^T \\ B & (-1/\lambda)C \end{bmatrix} \begin{bmatrix} u \\ p \end{bmatrix} = \begin{bmatrix} f \\ 0 \end{bmatrix}, \quad (3.1)$$

corresponding to a stable, mixed finite element formulation of the elasticity problem on a subdomain Ω_i ; to simplify, we work without the index i in this section. From (2.3) and with A the stiffness matrix corresponding to $a_i(\cdot, \cdot)$, etc., we find

$$(p^T B u)^2 \leq (n/2)(u^T A u)(p^T C p). \quad (3.2)$$

Setting $p = \lambda C^{-1}Bu$ in (3.2) then gives, after canceling a common factor,

$$u^T B^T C^{-1}Bu \leq (n/2)u^T Au. \quad (3.3)$$

We note that $u^T B^T C^{-1}Bu$ can also be written as $\int_{\Omega_i} |\operatorname{div} \mathbf{u}|^2 dx$.

The energy of u is defined as $u^T \tilde{A}u$, where

$$\tilde{A} = \mu A + \lambda B^T C^{-1}B, \quad (3.4)$$

a Schur complement obtained by eliminating the variable p ; we will also work with a bilinear form $\tilde{a}_i(\cdot, \cdot)$ which corresponds to this displacement-only formulation. We next partition the displacement vector into

$$u = \begin{bmatrix} u_I \\ u_\Gamma \end{bmatrix}. \quad (3.5)$$

Here the subscripts I and Γ refer to internal and interface, respectively, and we see that (3.1) can be expressed equivalently as

$$\begin{bmatrix} \mu A_{II} & \mu A_{I\Gamma} & B_I^T \\ \mu A_{\Gamma I} & \mu A_{\Gamma\Gamma} & B_\Gamma^T \\ B_I & B_\Gamma & (-1/\lambda)C \end{bmatrix} \begin{bmatrix} u_I \\ u_\Gamma \\ p \end{bmatrix} = \begin{bmatrix} f_I \\ f_\Gamma \\ 0 \end{bmatrix}. \quad (3.6)$$

For p with zero mean, we obtain from (2.4), and a standard argument,

$$p^T B_I A_{II}^{-1} B_I^T p \geq \beta^2 p^T C p, \quad (3.7)$$

where β is the discrete inf-sup constant.

From the divergence theorem, we have

$$\int_{\Omega_i} \operatorname{div} \mathbf{u} dx = \int_{\partial\Omega_i} (\mathbf{u} \cdot \mathbf{n}) dS = g^T u_\Gamma, \quad (3.8)$$

where \mathbf{n} is the unit outward normal for $\partial\Omega_i$, and g is a constant vector associated with the flux of \mathbf{u} across $\partial\Omega_i$. We will use a vector of constant divergence defined by

$$\mathbf{v} = \frac{g^T u_\Gamma}{n|\Omega_i|} \sum_{j=1}^n x_j \mathbf{e}_j, \quad (3.9)$$

where x_j and \mathbf{e}_j are the coordinate and unit vector, respectively, for direction j . We also find that

$$\int_{\Omega_i} \operatorname{div} \mathbf{v} dx = \int_{\Omega_i} \operatorname{div} \mathbf{u} dx. \quad (3.10)$$

Consequently, since $\operatorname{div} \mathbf{v}$ is a constant,

$$(\lambda/|\Omega_i|)v_\Gamma^T g g^T v_\Gamma = \lambda \int_{\Omega_i} |\operatorname{div} \mathbf{v}|^2 dx \leq \lambda \int_{\Omega_i} |\operatorname{div} \mathbf{u}|^2 dx \quad (3.11)$$

and

$$g^T v_\Gamma = \int_{\partial\Omega_i} (\mathbf{v} \cdot \mathbf{n}) dS = \int_{\partial\Omega_i} (\mathbf{u} \cdot \mathbf{n}) dS = g^T u_\Gamma. \quad (3.12)$$

Furthermore, by (3.3),

$$\begin{aligned} u^T(A/2)u &= \int_{\Omega_i} \epsilon(\mathbf{u}) : \epsilon(\mathbf{u}) \, dx \geq (1/n) \int_{\Omega_i} |\operatorname{div} \mathbf{u}|^2 \, dx \\ &\geq (1/n) \int_{\Omega_i} |\operatorname{div} \mathbf{v}|^2 \, dx \\ &= \int_{\Omega_i} \epsilon(\mathbf{v}) : \epsilon(\mathbf{v}) \, dx, \end{aligned} \quad (3.13)$$

and we obtain

$$v^T A v \leq u^T A u \quad (3.14)$$

and

$$v^T \tilde{A} v = \frac{\lambda + 2\mu}{|\Omega_i|} u_\Gamma^T g g^T u_\Gamma \leq u^T \tilde{A} u. \quad (3.15)$$

Now let

$$w_\Gamma = u_\Gamma - v_\Gamma; \quad (3.16)$$

it follows that $g^T w_\Gamma = 0$, i.e., the net flux across $\partial\Omega_i$ of w_Γ is zero.

We return to (3.6) for (w, q) , and consider the case with $f_I = 0$ and w_Γ given. We then obtain

$$\begin{bmatrix} \mu A_{II} & B_I^T \\ B_I & (-1/\lambda)C \end{bmatrix} \begin{bmatrix} w_I \\ q \end{bmatrix} = \begin{bmatrix} -\mu A_{I\Gamma} w_\Gamma \\ -B_\Gamma w_\Gamma \end{bmatrix}. \quad (3.17)$$

In addition, the mean value of q is zero as a consequence of $g^T w_\Gamma = 0$ and the divergence theorem. Although B_I is rank deficient with a null space of dimension 1, the linear system in (3.17) is consistent even for $1/\lambda = 0$ since the mean value of q is zero. Elimination of w_I gives

$$((\mu/\lambda)C + B_I A_{II}^{-1} B_I^T) q = \mu(B_\Gamma - B_I A_{II}^{-1} A_{I\Gamma}) w_\Gamma, \quad (3.18)$$

and it then follows from (3.17) and (3.18) that

$$w^T \tilde{A} w = \mu w_\Gamma^T S_{\Gamma\Gamma} w_\Gamma + \mu w_\Gamma^T \tilde{B}_\Gamma S_{\mu,\lambda}^{-1} \tilde{B}_\Gamma w_\Gamma, \quad (3.19)$$

where

$$S_{\Gamma\Gamma} = A_{\Gamma\Gamma} - A_{\Gamma I} A_{II}^{-1} A_{I\Gamma}, \quad \tilde{B}_\Gamma = B_\Gamma - B_I A_{II}^{-1} A_{I\Gamma}, \quad (3.20)$$

and

$$S_{\mu,\lambda} = (\mu/\lambda)C + B_I A_{II}^{-1} B_I^T. \quad (3.21)$$

We will use minimal energy extensions with respect to \tilde{A} and A .

DEFINITION 3.1. *The discrete saddle-point harmonic function for boundary data w_Γ has the vector representation*

$$w_{sh} = \begin{bmatrix} w_I \\ w_\Gamma \end{bmatrix},$$

where w_I is given by the solution of (3.17).

DEFINITION 3.2. *The discrete harmonic function for boundary data w_Γ has the vector representation*

$$\hat{w} = \begin{bmatrix} -A_{II}^{-1}A_{I\Gamma} \\ I \end{bmatrix} w_\Gamma.$$

We can then rewrite (3.19) as

$$w^T \tilde{A}w = \mu \hat{w}^T A \hat{w} + \mu \hat{w}^T B^T S_{\mu,\lambda}^{-1} B \hat{w}. \quad (3.22)$$

It then follows from (3.3), (3.7), and the definition of $S_{\mu,\lambda}$, that

$$w^T \tilde{A}w \leq \left(1 + \frac{n/2}{\mu/\lambda + \beta^2}\right) \mu \hat{w}^T A \hat{w}. \quad (3.23)$$

Therefore, the energy of the discrete saddle-point harmonic function for the boundary data w_Γ is bounded by a constant times that of the discrete harmonic function with respect to the μA norm. This result will allow us to work with the benign μA norm, even as λ approaches infinity, for displacement fields which satisfy a no net flux condition. For general displacement fields, we have.

LEMMA 3.3. *Let u_{sh} denote the discrete saddle-point harmonic function with the same boundary data u_Γ as u . Then,*

$$u_{sh}^T \tilde{A}u_{sh} \leq 4 \left(1 + \frac{n/2}{\mu/\lambda + \beta^2}\right) \mu u^T A u + \frac{2(\lambda + 2\mu)}{|\Omega_i|} u_\Gamma^T g g^T u_\Gamma \quad (3.24)$$

Proof. With $u = v + w$, we find, by using (3.23), (3.16), and (3.14), that

$$\begin{aligned} u^T \tilde{A}u &\leq 2(v^T \tilde{A}v + w^T \tilde{A}w) \\ &\leq 2(v^T \tilde{A}v + (1 + (n/2)/(\mu/\lambda + \beta^2))\mu \hat{w}^T A \hat{w}) \\ &\leq 2(v^T \tilde{A}v + 2(1 + (n/2)/(\mu/\lambda + \beta^2))\mu(v^T A v + u^T A u)) \\ &\leq 4(1 + (n/2)/(\mu/\lambda + \beta^2))\mu u^T A u + 2(\lambda + 2\mu)/|\Omega_i| u_\Gamma^T g g^T u_\Gamma. \end{aligned} \quad (3.25)$$

The lemma then follows from observing that $u_{sh}^T \tilde{A}u_{sh} \leq u^T \tilde{A}u$, since u_{sh} minimizes the energy with respect to \tilde{A} for the boundary data u_Γ . \square

4. The algorithm and the main result. We will describe and analyze our algorithm as a two-level Schwarz method, as in [33, Chapters 2 and 3], defined in terms of a set of subspaces. To simplify the discussion, we will consider only the case when exact solvers are used for both the coarse problem and the local problems. We will work with the displacement variables only and with the positive definite formulation obtained after all pressure degrees of freedom have been eliminated. We will use a coarse space \mathbf{V}_0 , and a number of local spaces \mathbf{V}'_i associated with an overlapping covering $\{\Omega'_i\}$ of Ω . We will assume that each Ω'_i is constructed by adding layers of elements to a subdomain Ω_i . While other recipes have been considered, this is the most popular approach. We also assume that all finite element nodes for the displacement, which belong to an element with at least one node on an edge of a subdomain Ω_i , belong to Ω'_i ; in case, we have interior nodes in the elements, as, e.g., for the Q_2 elements, we can relax this condition and only require that we have at least one additional layer of elements in the extended subdomain Ω'_i .

The overlap between the subdomains is characterized by parameters δ_i , somewhat differently from [33, Assumption 3.1]: δ_i is the minimum width of the neighborhood $\Omega_{i,\delta_i} \subset \Omega_i$ of $\partial\Omega_i$ that is also covered by neighboring overlapping subdomains Ω'_j , $j \neq i$.

The coarse component space of our preconditioner is adapted from an earlier iterative substructuring algorithm [33, Algorithm 5.16] first developed for scalar elliptic problems in [17]. Because of the larger null space of the elasticity operator, we need to enrich that coarse space to make it work for elasticity. This is related to the well-known null space property, which is necessary to obtain scalability, i.e., a bound on the convergence, which does not depend on the number of subdomains; see the discussion in [29] or [31]. We build the local components of our preconditioner by restricting the original problem to the overlapping subdomains Ω'_i .

To introduce the coarse space \mathbf{V}_0 , we first decompose the interface Γ . For problems in the plane, the interface is the union of edges and vertices. An edge \mathcal{E}^{ij} is an open subset of $\Gamma_i := \partial\Omega_i \cap \Gamma$, which contains all nodes which are shared by the boundaries of only a pair of subdomains Ω_i and Ω_j . The subdomain vertices $\mathcal{V}^{i\ell}$ are endpoints of edges and typically are shared by more than two subdomains.

In three dimensions, Γ_i is the union of faces \mathcal{F}^{ij} , edges \mathcal{E}^{ik} , and vertices $\mathcal{V}^{i\ell}$. A node on a face is common to two subdomains Ω_i and Ω_j while those on an edge typically are common to more than two.

We can think of each of these sets in terms of an equivalence class of finite element nodes. The class of a node $x \in \Gamma$ is determined by the set of subdomains with x in their closures. We note that for subdomains obtained from a mesh partitioner, the situation can be complicated and greater care with the definitions may be required, see, e.g., [26, Section 3] and [24].

All elements of the coarse space are discrete saddle-point harmonic functions, in the sense of Definition 3.1, and are therefore determined solely by their values on the interface and are of minimal elastic energy.

In the plane, we introduce an edge cutoff functions $\theta_{\mathcal{E}^{ij}}$ for each edge. It is a finite element function which equals 1 at all nodes of \mathcal{E}^{ij} and vanishes at all other interface nodes. They are complemented by vertex cutoff functions $\theta_{\mathcal{V}^{i\ell}}$ which equal 1 at the vertex and vanish at all other interface nodes. Together these functions form a partition of unity. For $n = 2$, we then obtain all the elements in our coarse space by using these functions and the rigid body modes,

$$\mathbf{r}_1 := \begin{bmatrix} 1 \\ 0 \end{bmatrix}, \mathbf{r}_2 := \begin{bmatrix} 0 \\ 1 \end{bmatrix}, \mathbf{r}_3 := \frac{1}{H_i} \begin{bmatrix} -x_2 + \hat{x}_2 \\ x_1 - \hat{x}_1 \end{bmatrix}.$$

Here \hat{x} is a suitable shift, e.g., to the middle of the edge, to make this basis well conditioned. The scaling $1/H_i$ ensures that the norms of the three functions are comparable.

The basis functions of our coarse space are obtained by multiplying these vector valued functions by $\theta_{\mathcal{E}^{ik}}$ and bringing them into the finite element space by interpolating using the values at the nodes on the interface. We can obtain the same basis elements by restricting the three rigid body modes to the nodes of the edge and setting the values at all other interface nodes to zero. For each edge, we thus obtain three basis functions. In addition, we have two degrees of freedom for each vertex $\mathcal{V}^{i\ell}$ representing its displacement.

A similar construction is used for the three-dimensional case. The rigid body

modes are now three translations

$$\mathbf{r}_1 := \begin{bmatrix} 1 \\ 0 \\ 0 \end{bmatrix}, \mathbf{r}_2 := \begin{bmatrix} 0 \\ 1 \\ 0 \end{bmatrix}, \mathbf{r}_3 := \begin{bmatrix} 0 \\ 0 \\ 1 \end{bmatrix}, \quad (4.1)$$

and three rotations

$$\mathbf{r}_4 := \frac{1}{H_i} \begin{bmatrix} 0 \\ -x_3 + \hat{x}_3 \\ x_2 - \hat{x}_2 \end{bmatrix}, \mathbf{r}_5 := \frac{1}{H_i} \begin{bmatrix} x_3 - \hat{x}_3 \\ 0 \\ -x_1 + \hat{x}_1 \end{bmatrix}, \mathbf{r}_6 := \frac{1}{H_i} \begin{bmatrix} -x_2 + \hat{x}_2 \\ x_1 - \hat{x}_1 \\ 0 \end{bmatrix}, \quad (4.2)$$

where $\hat{x} \in \Omega_i$ can be chosen as a midpoint of an edge or face. The shift of the origin makes this basis for the space of rigid body modes well conditioned, and the scaling and shift make these six functions scale in the same way with H_i .

For each face, we can use a cutoff function $\theta_{\mathcal{F}^{ij}}$ or we can obtain six linearly independent basis functions by restricting the rigid body modes to the nodes of \mathcal{F}^{ij} and setting the values at all other interface nodes to zero. For a straight edge, on the other hand, we only obtain five, since as is easy to see, a rigid body mode representing a rotation with the edge as its axis, is invisible on the edge; for a detailed discussion of the case of curved edges, see [24] and also Section 6. For each vertex, finally, we have three degrees of freedom representing the displacement at that point.

It is clear from our construction that, when restricted to an interior subdomain, this coarse space will contain all the rigid body modes. As previously noted, this is a requirement for obtaining a scalable algorithm, see also [33, Section 8.2].

As previously indicated, the local components of the preconditioner are based on a set of overlapping subdomains $\{\Omega'_i\}$. Each of them is associated with a bilinear form $\tilde{a}'_i(\cdot, \cdot)$ obtained by integrating only over Ω'_i in (2.2), and then eliminating the pressure variables, i.e., this bilinear form corresponds to the displacement-only formulation. For the local problems, we use zero Dirichlet data on $\partial\Omega'_i$. Thus, our local spaces $\mathbf{V}'_i, i = 1, \dots, N$, are defined as

$$\mathbf{V}'_i = \mathbf{V}^h(\Omega'_i) \cap \mathbf{H}_0^1(\Omega'_i). \quad (4.3)$$

This is the standard choice as in [33, Chapter 3].

All that is now required for the analysis of our algorithm is an estimate of a parameter in a stable decomposition of any element in the finite element space; see [33, Assumption 2.2 and Lemma 2.5]. We need to estimate C_0^2 in

$$\tilde{a}(\mathbf{u}_0, \mathbf{u}_0) + \sum_{j=1}^N \tilde{a}'_j(\mathbf{u}_j, \mathbf{u}_j) \leq C_0^2 \tilde{a}(\mathbf{u}, \mathbf{u}) \quad \forall \mathbf{u} \in \mathbf{V}^h, \quad (4.4)$$

for some choice of $\{\mathbf{u}_i\}_0^N$, such that

$$\mathbf{u} = \sum_{j=0}^N R_j^T \mathbf{u}_j, \quad \mathbf{u}_i \in \mathbf{V}'_i. \quad (4.5)$$

Here, $\tilde{a}(\cdot, \cdot)$ is the displacement-only bilinear form for the entire domain Ω . For $i \geq 1$, we use the extension operators $R_i^T : \mathbf{V}'_i \rightarrow \mathbf{V}^h$. Similarly, R_0^T imbeds \mathbf{V}_0 into \mathbf{V}^h .

Associated with the coarse space is a projection $P_0 : \mathbf{V}^h \rightarrow \mathbf{V}_0$; it is orthogonal with respect to the $\tilde{a}(\cdot, \cdot)$ -inner product. For each local space \mathbf{V}'_i , there is a projection P_i defined by

$$P_i = R_i^T \tilde{P}_i \quad \text{with } \tilde{P}_i \text{ defined by } \tilde{a}'_i(\tilde{P}_i \mathbf{u}, \mathbf{v}) = \tilde{a}(\mathbf{u}, R_i^T \mathbf{v}) \quad \forall \mathbf{v} \in \mathbf{V}'_i.$$

The additive Schwarz operator, the preconditioned operator used in our iteration, is given by

$$P_{ad} = \sum_{j=0}^N P_j.$$

By using [33, Lemmas 2.5 and 2.10], we find that the condition number $\kappa(P_{ad})$ can be bounded by $(N^C + 1)C_0^2$ where N^C is the minimal number of colors required to color the subdomains Ω'_i such that no pair of intersecting subdomains have the same color.

Our main result is:

THEOREM 4.1 (Condition number estimate). *The condition number of our domain decomposition method satisfies*

$$\kappa(P_{ad}) \leq C(1 + (H/\delta))^3(1 + \log(H/h))^2,$$

where C is a constant, independent of the number of subdomains and their diameters and the mesh size and which only depends on the number of colors required for the overlapping subdomains and the shape regularity of the elements and the subdomains.

As in many domain decomposition results, H/h is shorthand for $\max_i(H_i/h_i)$, where h_i is the smallest diameter of the elements of Ω_i . Similarly, H/δ is the largest ratio of H_i and δ_i .

By using [33, Theorem 2.9], we can obtain a similar result for multiplicative Schwarz methods.

5. Proof of main result. Our proof is in three parts. As just indicated, we need to estimate the parameter C_0^2 of (4.4). To do so, we first design a coarse component \mathbf{u}_0 and provide a bound on $\tilde{a}(\mathbf{u}_0, \mathbf{u}_0)$ by estimating $\tilde{a}_i(\mathbf{u} - \mathbf{u}_0, \mathbf{u} - \mathbf{u}_0)$. The coarse interpolant \mathbf{u}_0 will be chosen so that we can estimate $\tilde{a}_i(\mathbf{u} - \mathbf{u}_0, \mathbf{u} - \mathbf{u}_0)$ in terms $a_i(\mathbf{u} - \mathbf{u}_0, \mathbf{u} - \mathbf{u}_0)$, by using Lemma 3.3, with a constant that does not grow with the parameter λ . In Subsection 5.3, we will similarly design and estimate the local components \mathbf{u}_i of a partition of \mathbf{u} as in (4.5) and we will again obtain a result which holds uniformly with respect to λ .

We can rely on some standard technical tools collected in [33, Section 4.6] and [26, Section 7]; they were developed for scalar elliptic problems and compressible elasticity, respectively. Thus, we can obtain estimates, in the norm defined by $a_i(\cdot, \cdot)$ in Section 2 and by the matrix A in Section 3, by using estimates in the $\mathbf{H}^1(\Omega_i)$ -norm and the elementary inequality

$$a_i(\mathbf{v}, \mathbf{v}) = 2 \int_{\Omega_i} \varepsilon(\mathbf{v}) : \varepsilon(\mathbf{v}) dx \leq 2|\mathbf{v}|_{\mathbf{H}^1(\Omega_i)}^2. \quad (5.1)$$

We can then return to the norm defined by $a_i(\cdot, \cdot)$ by using the second Korn inequality:

LEMMA 5.1. (*Korn's second inequality*) *Let Ω_i be a Lipschitz domain of diameter H_i . Then, there exists a constant $C = C(\Omega_i)$ such that*

$$\|\mathbf{v}\|_{\mathbf{H}^1(\Omega_i)}^2 \leq C(a_i(\mathbf{v}, \mathbf{v}) + \frac{1}{H_i^2}\|\mathbf{v}\|_{L^2(\Omega_i)}^2).$$

The norm of the left hand side is the scaled \mathbf{H}^1 -norm:

$$\|\mathbf{v}\|_{\mathbf{H}^1(\Omega_i)}^2 := |\mathbf{v}|_{\mathbf{H}^1(\Omega_i)}^2 + \frac{1}{H_i^2}\|\mathbf{v}\|_{L^2(\Omega_i)}^2.$$

We note that the constant C in Lemma 5.1 depends on the shape regularity of the subdomain, but that we will only need this result for the subdomains Ω_i , which, by assumption, are shape regular. In Subsections 5.2 and 5.3, we will face other issues concerning domains with poor aspect ratios, when we consider the inf-sup parameter, and bounds which depend on the aspect ratio will be part of the proof of our main result. We also note that inf-sup stability and Korn's second inequality are closely related; see, e.g., Bramble [6] in which new proofs of both results are given for general Lipschitz domains.

By using Lemma 5.1 and a Poincaré inequality, we obtain

LEMMA 5.2. *Let Ω_i be a Lipschitz domain of diameter H_i . Then, there exists a constant $C = C(\Omega_i)$ such that*

$$\inf_{\mathbf{r} \in \mathcal{RB}} \|\mathbf{v} - \mathbf{r}\|_{\mathbf{H}^1(\Omega_i)}^2 \leq C a_i(\mathbf{v}, \mathbf{v}).$$

Here \mathcal{RB} is the space of rigid body modes.

In a final, elementary step of our proof, we will use that $\mu a_i(\mathbf{v}, \mathbf{v}) \leq \tilde{a}_i(\mathbf{v}, \mathbf{v})$.

We recall that \mathbf{u}_0 and indeed all elements of the coarse space are discrete saddle-point harmonic functions. Therefore $\tilde{a}(\mathbf{u}_0, \mathbf{u}_0) \leq \tilde{a}(\mathbf{v}, \mathbf{v})$ for any \mathbf{v} which equals \mathbf{u}_0 on the interface Γ . Therefore, in the different steps of our proof, we can work with any extension into the interior of the subdomains which is convenient for us. We will focus on the more difficult case of $n = 3$ since no additional ideas are required for the case of $n = 2$.

5.1. The coarse component of the decomposition. As in the theory for iterative substructuring algorithms, see [33, Chapters 4, 5, and 6], the analysis can be carried out for one subdomain Ω_i at a time and variations in the values of the Lamé parameters between subdomains will therefore not enter our bounds.

We recall that the coarse space, restricted to an individual subdomain that does not touch $\partial\Omega$, will contain all rigid body modes and that we have constructed a basis for the coarse space in terms of these modes and cutoff functions associated with the faces, edges, and vertices of the subdomain Ω_i . When constructing the coarse space component \mathbf{u}_0 , by a specific interpolation procedure, we will make sure that all rigid body modes are reproduced and also that the remainder, $\mathbf{w} = \mathbf{u} - \mathbf{u}_0$, will have a zero net flux across all the faces of the interface. Our construction and estimates can be used both for interior subdomains and for those with a boundary that intersects $\partial\Omega$; our interpolation procedure will reproduce the zero Dirichlet boundary condition on $\partial\Omega_i \cap \partial\Omega$.

The construction of \mathbf{u}_0 begins by setting $\mathbf{u}_0(\mathcal{V}^{i\ell}) = \mathbf{u}(\mathcal{V}^{i\ell})$ at all vertices of the subdomain.

Next, for each edge $\mathcal{E}^{j\ell} \subset \partial\Omega_i$, common to two faces \mathcal{F}^{ij} and $\mathcal{F}^{i\ell}$, we select the coefficients for the edge basis elements such that

$$(\mathbf{u} - \mathbf{u}_0, \mathbf{r})_{L^2(\mathcal{E}^{j\ell})} = 0 \quad \forall \mathbf{r} \in \mathcal{RB}.$$

We note that, since an edge component is obtained by restricting rigid body modes to the nodes of the edge and $\mathbf{u} - \mathbf{u}_0$ vanishes at the subdomain vertices, we can also find that component by solving

$$\inf_{\mathbf{r} \in \mathcal{RB}} \|I^h(\theta_{\mathcal{E}^{j\ell}}(\mathbf{u} - \mathbf{r}))\|_{L^2(\mathcal{E}^{j\ell})}^2. \quad (5.2)$$

Here, I^h is the interpolation operator that maps any continuous function into the finite element space \mathbf{V}^h . By using (5.2), we obtain

$$\|I^h(\theta_{\mathcal{E}^{j\ell}}(\mathbf{u} - \mathbf{u}_0))\|_{L^2(\mathcal{E}^{j\ell})} \leq \|I^h(\theta_{\mathcal{E}^{j\ell}}(\mathbf{u} - \mathbf{r}))\|_{L^2(\mathcal{E}^{j\ell})} \quad \forall \mathbf{r} \in \mathcal{RB}. \quad (5.3)$$

The $\mathbf{H}^1(\Omega_i)$ -norm of the edge contributions can be estimated in terms of the norm in $L^2(\mathcal{E}^{j\ell})$ by using [33, Lemma 4.19]. Similarly, the $L^2(\mathcal{E}^{j\ell})$ -norm can be estimated by the $\mathbf{H}^1(\Omega_i)$ -norm by using [33, Lemma 4.16]. Using Lemma 5.2, we then find that

$$\begin{aligned} \inf_{\mathbf{r} \in \mathcal{RB}} \|I^h(\theta_{\mathcal{E}^{j\ell}}(\mathbf{u} - \mathbf{r}))\|_{L^2(\mathcal{E}^{j\ell})}^2 &\leq \inf_{\mathbf{r} \in \mathcal{RB}} C \|\mathbf{u} - \mathbf{r}\|_{L^2(\mathcal{E}^{j\ell})}^2 \\ &\leq C(1 + \log(H/h)) \inf_{\mathbf{r} \in \mathcal{RB}} \|\mathbf{u} - \mathbf{r}\|_{\mathbf{H}^1(\Omega_i)}^2 \leq C(1 + \log(H/h)) a_i(\mathbf{u}, \mathbf{u}). \end{aligned}$$

Finally, for each face, $\mathcal{F}^{ij} \subset \partial\Omega_i$, we similarly select the coefficients for the face basis functions such that

$$(\mathbf{u} - \mathbf{u}_0, \mathbf{r})_{L^2(\mathcal{F}^{ij})} = 0 \quad \forall \mathbf{r} \in \mathcal{RB}. \quad (5.4)$$

An estimate of the contribution from a face to \mathbf{u}_0 requires more work since we need to take into account, not only of \mathbf{u} , but also of the edge contributions to \mathbf{u}_0 that were just considered; the values at the vertices, on the other hand, will not enter the computation. The contribution from the face \mathcal{F}^{ij} to \mathbf{u}_0 is the discrete saddle-point harmonic function with the same boundary values as $I^h(\theta_{\mathcal{F}^{ij}} \mathbf{r}')$, for some $\mathbf{r}' \in \mathcal{RB}$.

To estimate the face contribution, we consider the linear system of equations, which determines the coefficients with respect to the basis for \mathcal{RB} , given in (4.1) and (4.2), of the contribution of the face to \mathbf{u}_0 . By using that we only have a six-by-six linear system and a well-conditioned basis, we can estimate these coefficients by

$$C/H_i (\|\mathbf{u}\|_{L^2(\mathcal{F}^{ij})} + \sqrt{h_i} \|\mathbf{u}\|_{L^2(\mathcal{E}^{j\ell})}).$$

By a small modification of the proof of [26, Lemma 7.1], and the fact that the basis elements \mathbf{r}_k are bounded, we find that

$$|I^h(\theta_{\mathcal{F}^{ij}} \mathbf{r}_k)|_{\mathbf{H}^1(\Omega_i)}^2 \leq C(1 + \log(H_i/h_i)) H_i \quad k = 1, \dots, 6.$$

Therefore,

$$|I^h(\theta_{\mathcal{F}^{ij}} \mathbf{r}')|_{\mathbf{H}^1(\Omega_i)}^2 \leq C(1 + \log(H_i/h_i)) \left(\frac{1}{H_i} \|\mathbf{u}\|_{L^2(\mathcal{F}^{ij})}^2 + \frac{h_i}{H_i} \sum_{\mathcal{E}^{jk} \subset \partial\mathcal{F}^{ij}} \|\mathbf{u}\|_{L^2(\mathcal{E}^{j\ell})}^2 \right).$$

By using an elementary trace theorem [30, Theorem 1.2], [33, Lemma 4.17], and that $(h/H) \log(H/h)$ is bounded, we find that $|\mathbf{u}_0|_{\mathbf{H}^1(\Omega_i)}^2 \leq C(1 + \log(H_i/h_i)) \|\mathbf{u}\|_{\mathbf{H}^1(\Omega_i)}^2$. We can therefore conclude that

$$|\mathbf{u} - \mathbf{u}_0|_{\mathbf{H}^1(\Omega_i)}^2 \leq C(1 + \log(H/h)) \|\mathbf{u}\|_{\mathbf{H}^1(\Omega_i)}^2. \quad (5.5)$$

Our recipe for \mathbf{u}_0 will clearly reproduce any rigid body mode. We can therefore replace the norm in the right hand side of (5.5) by $\inf_{\mathbf{r} \in \mathcal{RB}} \|\mathbf{u} - \mathbf{r}\|_{\mathbf{H}^1(\Omega_i)}^2$. We can then use Lemma 5.2 and replace the square of the norm on the right hand side of (5.5) by $a_i(\mathbf{u}, \mathbf{u})$.

For flat faces, the condition (5.4) will make the net flux $\int_{\mathcal{F}^{ij}} \mathbf{w} \cdot \mathbf{n} \, dA$, of $\mathbf{w} = \mathbf{u} - \mathbf{u}_0$, vanish for each face separately, since the normal vector \mathbf{n} is then constant and

can be represented exactly as a translation. The case of curved faces will be discussed in Section 6.

We now consider $\tilde{a}_i(\mathbf{u} - \mathbf{u}_0, \mathbf{u} - \mathbf{u}_0)$. Since the net flux across $\partial\Omega_i$ of $\mathbf{u} - \mathbf{u}_0$ vanishes, we can use Lemma 3.3 and estimate this energy by

$$4 \left(1 + \frac{n/2}{\mu/\lambda + \beta^2} \right) \mu a_i(\mathbf{u} - \mathbf{u}_0, \mathbf{u} - \mathbf{u}_0).$$

This expression, in turn, can be estimated by

$$8 \left(1 + \frac{n/2}{\mu/\lambda + \beta^2} \right) \mu |\mathbf{u} - \mathbf{u}_0|_{\mathbf{H}^1(\Omega_i)}^2$$

and therefore, by using (5.5), also by $C(1 + \log(H_i/h_i))\mu a_i(\mathbf{u}, \mathbf{u})$. We can then return to the \tilde{a}_i -norm by using the elementary inequality $\mu a_i(\mathbf{u}, \mathbf{u}) \leq \tilde{a}_i(\mathbf{u}, \mathbf{u})$.

A bound,

$$\tilde{a}(\mathbf{u}_0, \mathbf{u}_0) \leq C(1 + \log(H/h))\tilde{a}(\mathbf{u}, \mathbf{u}),$$

now results by adding the contributions from all the subdomains.

5.2. The influence of aspect ratios on certain bounds. Before we turn to the analysis of the local terms, we formulate two results on the effect of the aspect ratios of domains on the inf-sup parameter and on a bound for a certain modified face function $\vartheta'_{\mathcal{F}^{ij}}$, which is supported in the closure of the intersection of $\Omega_i \cup \mathcal{F}^{ij} \cup \Omega_j$ and $\Omega'_i \cap \Omega'_j$. We will also consider

$$\Psi_{i\ell} := \bigcap_{m \in I_{i\ell}} \Omega'_m,$$

the intersection of the extensions Ω'_m of all subdomains Ω_m , which have the edge $\mathcal{E}^{i\ell}$ in common with Ω_i . Here, the set of subdomain indices is denoted by $I_{i\ell}$; we include i in this set.

Bounds over these domains, which have aspect ratios of order H/δ , will affect the estimates of the $\mathbf{u}_i \in \mathbf{V}'_i$, $i \geq 1$, in the decomposition of our estimate of C_0 , the parameter in (4.4), but, as previously noted, they are not needed for the coarse space component \mathbf{u}_0 since all estimates required in Subsection 5.1 are for entire subdomains which, by assumption, are shape regular.

We first consider the inf-sup parameter. This question has been considered in the literature, in particular, by Dobrowolski [12]. As in that paper, which concerns the continuous problem, we consider a domain Ω and an $\alpha \in \mathbb{R}^n$ with

$$1 = \alpha_1 \leq \alpha_i \leq \alpha_n, \quad 1 \leq i \leq n.$$

A stretched domain is then defined by

$$\Omega_\alpha = \{y \in \mathbb{R}^n : (y_1/\alpha_1, \dots, y_n/\alpha_n) \in \Omega\}.$$

Additional geometric parameters d_i , the diameter of Ω with respect to the coordinate directions, are defined by

$$d_i = \sup\{h : x, x + he_i \in \Omega\}, \quad 1 \leq i \leq n.$$

For our application, the following result will provide a bound on β , which decreases no faster than linearly in δ/H for the domains mentioned above and further considered in Subsection 5.3.

LEMMA 5.3. [*Dobrowolski*] *The inf-sup parameter $\beta(\Omega_\alpha)$ of the stretched domain satisfies*

$$\frac{\beta(\Omega)}{\alpha_n} \leq \beta(\Omega_\alpha) \leq \frac{C}{\alpha_n},$$

where $C^2 = d_1^3 d_2 \dots d_n / d^{n+2}$ and d is the length of the side of the largest n -cube that is contained in Ω .

To obtain the same result as in Lemma 5.3, for the discrete case, we combine this lemma with techniques developed in Stenberg [32]. We note that his arguments are in terms of macro-elements, i.e., local arguments are sufficient. Therefore, the aspect ratio of the domain enters only through the inf-sup parameter for the continuous problem.

One of the standard tools in the theory for iterative substructuring problems is provided by [33, Lemmas 4.23 and 4.24].

$$|I^h(\vartheta_{\mathcal{F}^{ij}} \mathbf{u})|_{\mathbf{H}^1(\Omega_i)}^2 \leq C(1 + \log(H_i/h_i))^2 \|\mathbf{u}\|_{\mathbf{H}^1(\Omega_i)}^2, \quad (5.6)$$

Here $\vartheta_{\mathcal{F}^{ij}}$ is an explicitly constructed function, which has the same boundary values as $\theta_{\mathcal{F}^{ij}}$ on Γ .

In our analysis of the local terms, we need a similar result but for the intersection of Ω_i with Ω'_j , the extension of the other subdomain Ω_j , which has a face \mathcal{F}^{ij} in common with Ω_i . The bound in the right hand side of (5.6) must then be multiplied by a factor H_i/δ_i .

LEMMA 5.4. *There exists a function $\vartheta'_{\mathcal{F}^{ij}}$, which is equal to 1 at the nodes on \mathcal{F}^{ij} and vanishes at all the nodes on the rest of the boundary of $\Omega_i \cap \Omega'_j$, such that*

$$|I^h(\vartheta'_{\mathcal{F}^{ij}} \mathbf{u})|_{\mathbf{H}^1(\Omega_i \cap \Omega'_j)}^2 \leq C(H_i/\delta_i)(1 + \log(H_i/h_i))^2 \|\mathbf{u}\|_{\mathbf{H}^1(\Omega_i)}^2. \quad (5.7)$$

We will prove this result for a square face and for a cube compressed in the direction normal to \mathcal{F}^{ij} , a domain which has dimensions $H_i \times H_i \times \delta_i$. We note that the result also holds for any domain which contains the compressed cube and shares this face with it; therefore, the boundary of the extended subdomains Ω'_j can be quite irregular. The proof can also easily be modified to hold for other geometric configurations such as a neighborhood of minimal thickness δ_i of a face of a tetrahedron. As we will see, we only need a positive lower bound for the interior angles at the edges of the face.

Proof. To establish (5.7), we need to examine and modify the proofs of [33, Lemmas 4.23 and 4.24]. Those proofs concern four functions $\vartheta_{\mathcal{F}^{ij}}$, one for each face of a shape regular tetrahedron.

An analogous construction for a cube is worked out in the doctoral thesis of Casarin [10, Subsection 3.3.2] and will now be outlined. While, in the proof of [33, Lemma 4.23], a tetrahedral subdomain is divided into four tetrahedra by connecting its vertices to its centroid, the cube is divided into six pyramids each with a face of the cube as its base. Similarly, to the tetrahedral case, these pyramids are each divided into four tetrahedra each with an edge selected from the edges of the cube and another connecting the centroid of the cube with the centroid of a face of the

cube that is adjacent to the first edge. The construction given below will show that functions $\vartheta_{\mathcal{F}^{ij}}$ can be constructed such that

$$|\nabla \vartheta_{\mathcal{F}^{ij}}(x)| \leq C/r,$$

where C is a constant and r the minimum distance of x to the wire basket of the cube.

In order to understand how this bound changes with the geometry, we will provide some further details. In the case of a cube, $\vartheta_{\mathcal{F}^{ij}}(x)$ is defined for all x , which are not on the wire basket of the cube, as follows: its values on the line segment between the centroid of the cube and the centroid of the face \mathcal{F}^{ij} varies linearly from $1/6$ to 1 . Similarly, the restriction of $\vartheta_{\mathcal{F}^{ij}}$ to the line segments between the centroid of the cube and the centroids of the other faces drops linearly from $1/6$ to 0 . The value elsewhere in each of the 24 tetrahedra is given by a constant value on any plane through the edge of the cube, which intersects one of the line segments just introduced, with its value determined by that on the line segment. In addition, $\vartheta_{\mathcal{F}^{ij}}(x)$ is set to 0 on the wire basket of the cube. The bound on the gradient of the function then follows easily.

We now examine the effect of shrinking the cube in the direction normal to the face \mathcal{F}^{ij} . With the new dimensions, $H_i \times H_i \times \delta_i$, the gradient of $\vartheta'_{\mathcal{F}^{ij}}$ can be estimated by $CH_i/r\delta_i$. This bound is the best possible for the four tetrahedra adjacent to the face and reflects the fact that the angle between two faces, of any subtetrahedron, which has an edge of the cube in common and is adjacent to \mathcal{F}^{ij} , shrinks by a factor $\arctan(\delta_i/H_i)$. On the other hand for the other tetrahedra adjacent to the edges of the face \mathcal{F}^{ij} , the angle in fact increases and the gradient decreases.

We also recall that the estimates of the energy of $\vartheta_{\mathcal{F}^{ij}} \mathbf{u}$, in the proof of [33, Lemmas 4.23 and 4.24], involves the introduction of cylindrical coordinates with individual edges of the cube as z -axes and integrating over individual subtetrahedra. The linear factor H_i/δ_i in (5.7) results from the fact that while the square of the gradient of $\vartheta'_{\mathcal{F}^{ij}}(x)$ grows quadratically in H_i/δ_i in the tetrahedra next to the face, the angle over which we integrate shrinks in proportion of δ_i/H_i . The bounds for the other twenty subtetrahedra pose no new difficulties. We also need a bound on the L_2 -norm of finite element functions over intervals of length H_i , which are parallel to edges of the cube, as in [33, Corollary 4.20]. We can use that bound directly by noting that the finite element functions are defined in all of Ω_i and by writing our bound, as in (5.7), in terms of the norm over the entire subdomain. \square

In the next subsection, we will find that our bounds will be proportional to $(H/\delta)^3$ with two of the factors originating from the inf-sup parameter and Lemmas 3.3 and 5.3 and one from the bound in Lemma 5.4.

5.3. The local components of the partitioning. The standard way of constructing and estimating the local components $\mathbf{u}_i \in \mathbf{V}'_i$ involves a partition of unity for all $x \in \Omega$; see [33, Sections 3.2 and 3.6]. Here, we adopt a different strategy. We will only consider the three-dimensional case.

We first remove the interior components of $\mathbf{w} = \mathbf{u} - \mathbf{u}_0$ for each subdomain; they vanish on the interface and are made orthogonal to the space of the discrete saddle-point harmonic functions defined in equation (3.17). Therefore, each of these interior functions can be bounded directly by the energy of \mathbf{w} contributed by an individual subdomain and they therefore contribute to the individual components \mathbf{u}_i in a harmless way. To simplify our notation, we will now denote by \mathbf{w} what remains after this correction.

We will now explore how the restriction \mathbf{w}_i of \mathbf{w} to Ω_i can be partitioned. For each face \mathcal{F}^{ij} , we will have contributions to \mathbf{u}_i and \mathbf{u}_j , and for each edge $\mathcal{E}^{i\ell}$, there will be contributions to $\mathbf{u}_m \forall m \in I_{i\ell}$. In all that follows, we will look exclusively at the contributions from Ω_i .

In preparation, we introduce an alternative discrete saddle-point harmonic edge cutoff function $\theta'_{\mathcal{E}^{i\ell}}$, which vanishes on the boundary of $\Psi_{i\ell}$. The dimension of this domain is on the order of $2\delta_i \times 2\delta_i \times H_i$ and $\theta'_{\mathcal{E}^{i\ell}}$ equals $\theta_{\mathcal{E}^{i\ell}}$ on the interface Γ . In fact, we will work out our estimate for a function $\vartheta'_{\mathcal{E}^{i\ell}}$, which is the zero extension of the values of $\theta'_{\mathcal{E}^{i\ell}}$ on the interface; cf. [33, Lemma 4.19].

We recall that $\mathbf{w} = \mathbf{u} - \mathbf{u}_0$ vanishes at all the vertices of the subdomains and that, by construction, the net flux across each face of the subdomain vanishes. We first decompose the restriction of \mathbf{w}_i to Γ_i into face and edge terms by using the cutoff functions $\vartheta'_{\mathcal{F}^{ij}}$ and $\vartheta'_{\mathcal{E}^{i\ell}}$. By Lemma 5.4, the $\mathbf{H}^1(\Omega_i)$ -energy of each of the resulting face terms can be bounded by $C(H_i/\delta_i)(1 + \log(H/h))^2 \|\mathbf{w}\|_{\mathbf{H}^1(\Omega_i)}^2$ and by [33, Lemmas 4.16 and 4.17], the energy of the edge terms can be bounded by $C(1 + \log(H/h)) \|\mathbf{w}\|_{\mathbf{H}^1(\Omega_i)}^2$. We note that the edge estimate does not require the factor H_i/δ_i , since the extension by zero provides a sharp bound; cf. [33, p. 103]. We will derive similar bounds on the \mathbf{u}_m into which \mathbf{w}_i will be partitioned.

While the trace of \mathbf{w}_i , by construction, will have a net zero flux across each face, this will generally no longer be true for $I^h(\vartheta'_{\mathcal{F}^{ij}} \mathbf{w})$ and the edge terms. We will therefore modify these face contributions and $I^h(\vartheta'_{\mathcal{E}^{i\ell}} \mathbf{w})$, the terms of the edges, to ensure that the net fluxes of the modified functions will vanish separately. This will make it possible to use Lemma 3.3.

For each face \mathcal{F}^{ij} and for each edge $\mathcal{E}^{i\ell}$ of that face, we identify the nodes on the face which are next to those of the edge; by assumption, they belong to $\Psi_{i\ell}$. For this face and this edge, we then construct a function $d_{i\ell} \mathbf{n}'_{i\ell}$ with a constant displacement $d_{i\ell}$ at those nodes, in the direction of the normal to the face \mathcal{F}^{ij} , and which vanishes at all other nodes of the closure of Ω_i . We choose the value of $d_{i\ell}$ so that

$$I^h(\vartheta'_{\mathcal{E}^{i\ell}} \mathbf{w}) - d_{i\ell} \mathbf{n}'_{i\ell}$$

has a zero net flux across the face \mathcal{F}^{ij} . The face function $I^h(\vartheta'_{\mathcal{F}^{ij}} \mathbf{w}_i)$ is then modified by adding one such correction term for each of the edges of the face resulting in a face function $\mathbf{w}_{\mathcal{F}^{ij}}$ with a zero net flux across \mathcal{F}^{ij} . Thus,

$$\mathbf{w}_{\mathcal{F}^{ij}} := I^h(\vartheta'_{\mathcal{F}^{ij}} \mathbf{w}_i) + \sum_{\mathcal{E}^{ik} \subset \partial \mathcal{F}^{ij}} d_{ik} \mathbf{n}'_{ik}.$$

Similarly, we define an edge function by

$$\mathbf{w}_{\mathcal{E}^{i\ell}} := I^h(\vartheta'_{\mathcal{E}^{i\ell}} \mathbf{w}) - d_{i\ell} \mathbf{n}'_{i\ell} - d_{ij} \mathbf{n}'_{ij}. \quad (5.8)$$

We note that third term represents a displacement in the direction of the normal to the face $\mathcal{F}^{i\ell}$ of Ω_i , which is also adjacent to the edge $\mathcal{E}^{i\ell}$, and that the coefficient d_{ij} is chosen so that there is a zero net flux across that face.

By using (5.3), it is easy to show that $|d_{ik}|^2 \leq (C/H_i) \|\mathbf{u} - \mathbf{r}\|_{L^2(\mathcal{E}^{i\ell})}^2$, for any $\mathbf{r} \in \mathcal{RB}$, and that the $\mathbf{H}^1(\Omega_i)$ -norm of each of the three terms of $\mathbf{w}_{\mathcal{E}^{i\ell}}$ can be estimated by

$$C(1 + \log(H_i/h_i)) \|\mathbf{u} - \mathbf{r}\|_{\mathbf{H}^1(\Omega_i)}^2 \quad \forall \mathbf{r} \in \mathcal{RB}.$$

We now show how to divide $\mathbf{w}_{\mathcal{F}^{ij}}$ into contributions to \mathbf{u}_i and \mathbf{u}_j , which are the contributions of \mathbf{V}'_i and \mathbf{V}'_j to the decomposition (4.5). We allocate $(1/2)\mathbf{w}_{\mathcal{F}^{ij}}$ to \mathbf{u}_j and, to start constructing \mathbf{u}_i , we subtract the same function from \mathbf{w}_i , the restriction of \mathbf{w} to the closure of Ω_i . With the same recipe used for Ω_j , the subdomain across the face \mathcal{F}^{ij} , we see that these contributions to \mathbf{u}_i and \mathbf{u}_j will be continuous. Each of them also has a zero net flux across $\partial\Omega_i$.

We then partition the edge function $\mathbf{w}_{\mathcal{E}^{i\ell}}$. We construct a saddle-point harmonic function supported in the closure of $\Psi_{i\ell}$ and with the same boundary data on $\partial\Omega_i$ as the edge function $\mathbf{w}_{\mathcal{E}^{i\ell}}$ given by (5.8). If p subdomains share the edge, we then divide this function by p and add it to the contributions from the faces to the $\mathbf{u}_m, m \neq i, m \in I_{i\ell}$. We also subtract these $p - 1$ contributions from \mathbf{u}_i , previously obtained from \mathbf{w}_i by subtracting $(1/2)\mathbf{w}_{\mathcal{F}^{ik}}$ for each face of Ω_i . We note that all the resulting \mathbf{u}_m will, by construction, satisfy the no net flux condition and that we maintain continuity across the interface.

By using the no net flux condition, Lemmas 5.3 and 3.3, and the aspect ratios of $\Omega_i \cap \Omega'_k$, we find that

$$\tilde{a}_i(\mathbf{u}_m, \mathbf{u}_m) \leq C(1 + (H_i/\delta_i))^2 a_i(\mathbf{u}_m, \mathbf{u}_m).$$

We now consider any of the contributions to \mathbf{u}_m , from the edges of Ω_i . By using the \mathbf{H}^1 -bounds just derived, they can be estimated by

$$C(1 + (H_i/\delta_i))^2 (1 + \log(H_i/h_i)) \tilde{a}_i(\mathbf{u}, \mathbf{u}).$$

By using (5.7), each of the face contributions can be estimated similarly, but with the larger factor $(1 + (H_i/\delta_i))^3 (1 + \log(H/h))^2$. The need for $(1 + \log(H_i/h_i))^2$ with a second logarithmic factor, which is missing in the estimates of Subsection 5.1, comes from an estimate of face terms such as $I^h(\vartheta'_{\mathcal{F}^{ij}} \mathbf{w})$ by using Lemma 5.4. The third power of $(1 + (H_i/\delta_i))$ also originates from Lemma 5.4. In the estimate of these face terms, we again can benefit from the fact that $I^h(\vartheta'_{\mathcal{F}^{ij}} \mathbf{w}) = I^h(\vartheta'_{\mathcal{F}^{ij}}(\mathbf{u} - \mathbf{r})) \forall \mathbf{r} \in \mathcal{RB}$. This follows from the fact that the restriction of \mathbf{u}_0 to \mathcal{F}^{ij} equals $I^h(\vartheta'_{\mathcal{F}^{ij}}(\mathbf{r}'))$ and that \mathbf{w} remains the same if we shift \mathbf{u} by any rigid body mode.

6. The effect of irregular subdomain boundaries. As we have seen, the assumptions that the subdomains are quite regular, cf. Subsection 2.2, makes it possible to use many technical tools, which have been used previously in many studies. This represented the state of the art of domain decomposition theory as of a couple of years ago. Thus, the same [33, Assumption 4.3] was used when obtaining many results on iterative substructuring algorithms given in Chapters 4–6 in that monograph. However, the subdomains are often generated by mesh partitioners such as METIS [21] and, in practice, there is no guarantee that the subdomains even be uniformly Lipschitz continuous. The subdomains are also likely to change quite considerably with changes in the mesh size and a repeated use of a mesh partitioner.

Recently, there has been considerable progress in developing new techniques, which require very limited regularity of the subdomain boundaries and with bounds which depend only on a few geometric parameters, which are easy to understand, see [15, 25]. These papers concern problems in the plane. We will find that our results in this paper can be extended to the same more general class of subdomains for the case of two dimensions. We will also explore the three-dimensional case. We note that the regularity of $\partial\Omega$, the boundary of the given domain, will play no role.

The minimal assumption used in the recent papers is that the subdomains are John domains.

DEFINITION 6.1 (John domain). *A domain $\Omega \subset \mathbb{R}^n$ – an open, bounded, and connected set – is a John domain if there exists a constant $C_J \geq 1$ and a distinguished central point $x_0 \in \Omega$ such that each $x \in \Omega$ can be joined to it by a rectifiable curve $\gamma : [0, 1] \rightarrow \Omega$ with $\gamma(0) = x_0$, $\gamma(1) = x$ and $|x - \gamma(t)| \leq C_J \cdot \text{distance}(\gamma(t), \partial\Omega)$ for all $t \in [0, 1]$.*

This condition can be viewed as a twisted cone condition. We note that certain snowflake curves with fractal boundaries are John domains. We note that the parameter C_J will depend on the aspect ratio as well as the boundary of the domain.

In many domain decomposition studies, an extension theorem is also required, see, e.g., [25]. An important extension theorem was established in [20] for all uniform domains. A uniform domain satisfies the John condition and can also have quite an irregular boundary such as that of a snowflake.

An important tool in the theory on domain decomposition algorithms is Poincaré’s inequality; see [15].

LEMMA 6.2 (Poincaré’s inequality). *Let Ω be a John domain. Then,*

$$\|u - \bar{u}_\Omega\|_{L_2(\Omega)}^2 \leq (\gamma(\Omega, n))^2 |\Omega|^{2/n} \|\nabla u\|_{L_2(\Omega)}^2 \quad \forall u \in H^1(\Omega).$$

Here the parameter $\gamma(\Omega, n)$ is the best parameter in an isoperimetric inequality

$$[\min(|A|, |B|)]^{1-1/n} \leq \gamma(\Omega, n) |\partial A \cap \partial B|. \quad (6.1)$$

Here, $A \subset \Omega$ is an arbitrary open set, $B = \Omega \setminus \bar{A}$, and $|A|$ is the measure of the set A , etc.

We note that it is known that any simply connected plane domain, with a finite parameter $\gamma(\Omega, 2)$, is a John domain; see [9]. It is also known, see [5], that any John domain has a bounded parameter $\gamma(\Omega, n)$.

In the present paper, the role of the Poincaré inequality is played by Lemma 5.2. This result has been established for uniform domains in [18] and a closely related result is given in [1] for John domains. Following [7, Lemma 11.2.3], we note that the inf-sup constant β , for the continuous problem, is the best constant in the estimate

$$\beta \|\mathbf{u}\|_{H^1(\Omega)} \leq \|p\|_{L_2(\Omega)}.$$

where \mathbf{u} is a solution of $\text{div } \mathbf{u} = p$ in $H_0^1(\Omega)$. This inequality has been established for John domains in [1]. The parameter β depends only on the John parameter C_J .

Reexamining Subsection 5.1 of this paper, we first note that the edge terms can be defined just as before by using (5.2). On the other hand, we find that condition (5.4) no longer will guarantee a zero net flux across curved faces. But, after having selected the vertex and edge contributions, we can select the face contribution for \mathcal{F}^{ij} by solving a variational problem with a single constraint

$$\inf_{\mathbf{r} \in \mathcal{RB}} \|I^h(\theta_{\mathcal{F}^{ij}}(\mathbf{r} - \mathbf{u}))\|_{L^2(\mathcal{F}^{ij})}^2, \quad \text{subject to} \quad \int_{\mathcal{F}^{ij}} (\mathbf{u} - \mathbf{u}_0) \cdot \mathbf{n} \, dA = 0.$$

It is easy to see that this approach will also reproduce any rigid body mode. We can also obtain bounds on the coefficients for \mathbf{u}_0 very similar to those in the proof of (5.5).

The two-dimensional case presents exactly the same issues.

A bound similar to (5.5) can be established for John domains in two dimensions. An additional factor of $(1 + \log(H/h))$, which does not affect the main result, has to be introduced, as in the proof of [15, Theorem 3.1], and for the same reason: a standard trace theorem is missing for general John domains and in our proof, a bound

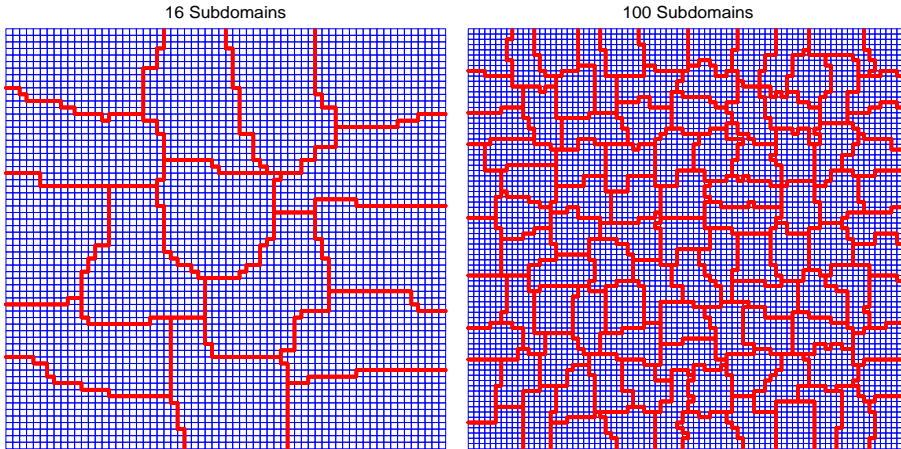


FIG. 7.1. *Examples of unstructured mesh decompositions used in numerical examples.*

on the L^∞ -norm of finite element functions is used; see [15, Lemma 3.2] for a proof for two-dimensional John domains. Estimates for edge cutoff functions, very similar to those for faces in this paper, are also known, see [25, Lemma 4.4]. By examining the rest of our proof in Section 5, we find that the main result of this paper also holds for the case of John subdomains in two dimensions.

For problems in three dimensions, the set of tools is still much less complete. One reason is that the John and uniform conditions then do not rule out that part of a middle of a face is very close to another face. This is unlikely to be a real issue in our application since, in Subsections 5.2 and 5.3, we work with domains which, by assumption, have a minimal thickness δ_i . Currently, a main open problem is to extend the bound in (5.6) under some appropriate geometric assumptions, which would be realistic for subdomains such as those generated by mesh partitioners.

7. Numerical Examples. Numerical examples are presented in this section for unit square domains in two dimensions (2D) and unit cube domains in three dimensions (3D). Homogeneous Dirichlet conditions are applied to the entire boundary in both cases. We consider both structured and unstructured mesh decompositions. For the structured decompositions, the subdomains are squares in 2D and cubes in 3D. For the unstructured decompositions, the graph partitioning software Metis [21] was used to decompose the mesh into N subdomains. Two examples of unstructured mesh decompositions are shown in Figure 7.1. All the examples used preconditioned conjugate gradients to solve the preconditioned linear system corresponding to the Schwarz operator P_{ad} to a relative residual tolerance of 10^{-8} for random right-hand-sides. Numbers of iterations (iter) and condition number estimates (cond) from the conjugate gradient iterations are reported in each of the tables.

7.1. Two Dimensions. Results for fixed values of $H/h = 8$ and $H/\delta = 4$ are shown in Table 7.1 for increasing numbers of subdomains N and three different values of Poisson ratio ν . As expected, condition number estimates appear to be bounded independently of both N and ν in the case of structured decompositions. We note that the same number of layers of additional elements were used for the overlapping subdomains for both types of mesh decompositions. Good scalability is also evident for unstructured decompositions, but there is more variability in the results. We

TABLE 7.1

Two dimensional results for $H/h = 8$, $H/\delta = 4$, and increasing numbers of subdomains N .

N	structured decomposition						unstructured decomposition					
	$\nu = 0.3$		$\nu = 0.4999$		$\nu = 0.49999$		$\nu = 0.3$		$\nu = 0.4999$		$\nu = 0.49999$	
	iter	cond	iter	cond	iter	cond	iter	cond	iter	cond	iter	cond
16	25	8.1	31	10.6	33	10.6	28	8.0	34	12.2	36	12.3
36	27	8.6	32	11.0	33	11.0	34	11.6	41	18.8	42	18.7
64	29	8.9	32	11.2	34	11.2	34	11.0	42	18.9	43	19.0
100	30	9.2	32	11.2	35	11.2	34	10.9	39	16.7	40	16.7
256*	32	9.7	34	11.6	35	11.7	38	12.6	44	23.1	45	23.1

TABLE 7.2

Two dimensional results for $N = 16$, $H/\delta = 4$, and increasing values of H/h .

H/h	structured decomposition						unstructured decomposition					
	$\nu = 0.3$		$\nu = 0.4999$		$\nu = 0.49999$		$\nu = 0.3$		$\nu = 0.4999$		$\nu = 0.49999$	
	iter	cond	iter	cond	iter	cond	iter	cond	iter	cond	iter	cond
8	25	8.05	31	10.6	33	10.6	29	8.71	34	14.3	34	14.3
16	27	8.89	33	12.3	34	12.3	33	11.4	40	18.1	41	18.2
32	28	9.67	35	14.1	36	14.1	29	8.18	34	12.8	34	12.8
64	30	10.4	36	15.8	38	15.8	33	9.89	38	16.0	40	16.1
128	31	11.0	38	17.4	40	17.4	33	9.76	40	18.1	41	18.1

note in the final row of Table 7.1 that the mesh was originally decomposed into 256 subdomains, but two of these subdomains had disconnected components which led to a total of 258 subdomains. Ideally, each subdomain would have 64 elements, but one of the subdomains had only 5 elements. Fortunately, the numerical results do not appear to be greatly sensitive to such imbalances.

The next example investigates the effect of increasing H/h while fixing $N = 16$ and $H/\delta = 4$. The results on the left side of Table 7.2 are also plotted in Figure 7.2. Notice that condition number estimates appear to be bounded by a constant times $1 + \log(H/h)$ for all values of ν . This bound is the same as the one for compressible elasticity (ν not too close to 0.5). These results suggest that it may be possible to remove one factor of $1 + \log(H/h)$ from the estimate in Theorem 4.1.

The next example investigates the effect of increasing H/δ while fixing $N = 16$ and $H/h = 120$. The results on the left side of Table 7.3 are also plotted in Figure 7.3. Notice that the results are fundamentally different for the compressible ($\nu = 0.3$) and almost incompressible cases. For compressible materials, condition number estimates appear to be proportional to H/δ , whereas for almost incompressible materials, the growth is much larger and closer to the estimate of $(H/\delta)^3$ in Theorem 4.1.

Another difference for compressible and almost incompressible materials is shown in Table 7.4. Here we see for a minimal overlap ($\delta/H = 0$) that the condition number estimates for almost incompressible materials grow without bound as the Poisson ratio approaches 0.5. Thus, for such materials, one should use an overlap no smaller than the element length h .

The next example is for a problem with discontinuous material properties. In a centered square region of length $1/2$, the elastic modulus $E = \sigma$ and the Poisson ratio $\nu = 0.3$. For the remaining part of the domain, $E = 1$ and $\nu = 0.49999$. For values of $\sigma \gg 1$, this can be viewed as a model of a steel component embedded in a softer, but almost incompressible, material such as rubber. Because the subdomain boundaries are aligned with material boundaries for the structured decomposition, condition number estimates in Table 7.5 are bounded independently of σ as the theory

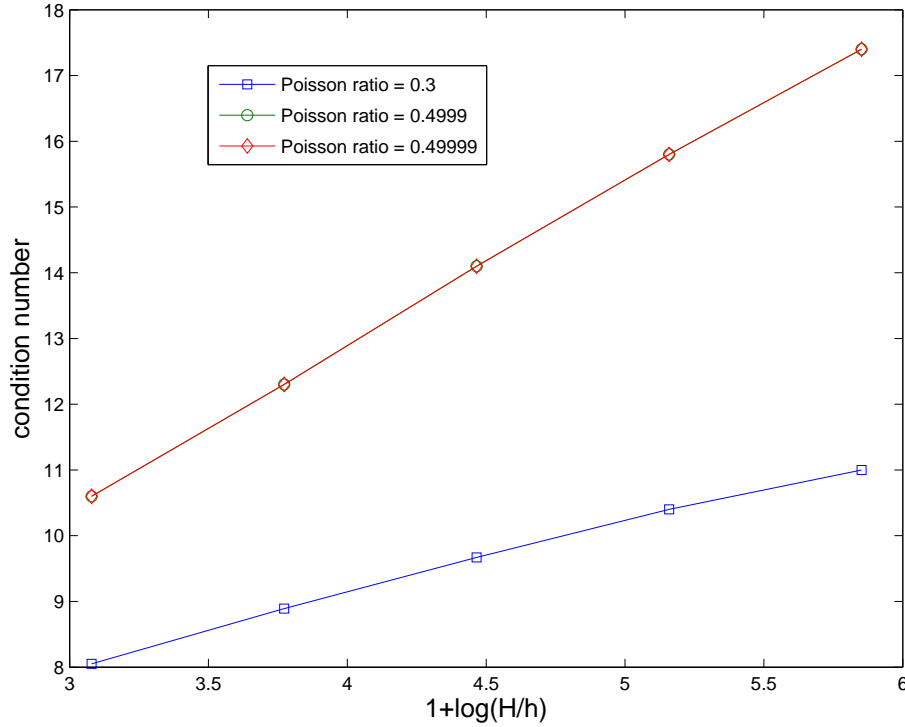


FIG. 7.2. Two dimensional results from Table 7.2.

TABLE 7.3

Two dimensional results for $N = 16$, $H/h = 120$, and increasing values of H/δ .

H/δ	structured decomposition				unstructured decomposition			
	$\nu = 0.3$		$\nu = 0.4999$		$\nu = 0.3$		$\nu = 0.4999$	
	iter	cond	iter	cond	iter	cond	iter	cond
4	31	11.0	37	17.2	33	9.61	38	16.2
5	33	11.9	39	19.3	35	10.5	40	19.0
6	34	12.6	42	21.0	36	11.4	43	21.3
10	39	14.9	50	32.4	41	14.4	52	33.8
12	41	16.3	57	42.9	43	15.8	59	45.5
15	44	18.4	70	69.3	45	19.1	71	71.9
20	48	21.8	98	142	49	20.8	90	121
30	56	31.9	163	424	56	28.5	144	317
40	63	42.1	> 200	945	64	37.3	> 200	673
60	75	62.4	> 200	2.83e3	78	55.1	> 200	2.02e3

TABLE 7.4

Two dimensional results for a structured decomposition of 16 subdomains with $H/h = 8$.

ν	$\delta/H = 1/4$		$\delta/H = 1/8$		$\delta/h = 0$	
	iter	cond	iter	cond	iter	cond
0.3	25	8.05	29	10.0	36	19.4
0.4	27	8.21	31	11.4	42	23.9
0.49	29	10.0	36	16.3	70	66.8
0.499	30	10.5	37	17.4	108	142
0.4999	31	10.6	39	17.6	> 200	526
0.49999	33	10.6	40	17.6	> 200	4.12e3

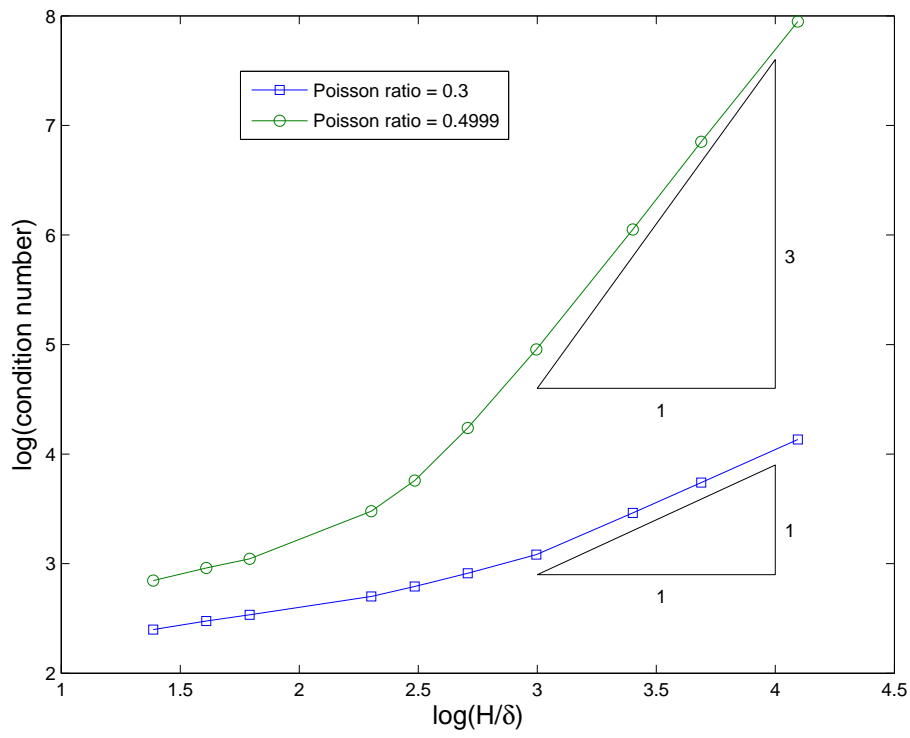


FIG. 7.3. Two dimensional results from Table 7.3.

TABLE 7.5

Two dimensional results for a problem with discontinuous material properties. Fixed values of $N = 16$, $H/h = 16$, and $H/\delta = 4$ are used.

σ	structured decomposition		unstructured decomposition	
	iter	cond	iter	cond
10^{-4}	35	10.3	36	11.0
10^2	34	10.3	34	10.7
1	36	11.7	35	11.9
10^2	34	14.7	40	25.4
10^4	32	14.9	43	149

TABLE 7.6

Three dimensional results for $H/h = 4$, $H/\delta = 4$, and increasing numbers of subdomains N . There was not enough memory available for $N = 216$ and the unstructured decomposition when run on a single processor.

N	structured decomposition						unstructured decomposition					
	$\nu = 0.3$		$\nu = 0.4999$		$\nu = 0.49999$		$\nu = 0.3$		$\nu = 0.4999$		$\nu = 0.49999$	
	iter	cond	iter	cond	iter	cond	iter	cond	iter	cond	iter	cond
27	32	13.7	40	19.7	40	19.7	35	13.2	44	22.6	47	22.6
64	34	15.3	42	21.3	45	21.3	37	14.3	46	23.6	47	23.7
125	35	16.3	46	22.8	47	22.9	40	16.0	48	24.8	51	24.8
216	37	17.1	46	23.9	50	24.1						

TABLE 7.7

Three dimensional results for $N = 27$, $H/\delta = 4$, and increasing values of H/h .

H/h	structured decomposition						unstructured decomposition					
	$\nu = 0.3$		$\nu = 0.4999$		$\nu = 0.49999$		$\nu = 0.3$		$\nu = 0.4999$		$\nu = 0.49999$	
	iter	cond	iter	cond	iter	cond	iter	cond	iter	cond	iter	cond
4	32	13.7	40	19.7	40	19.7	35	12.9	43	21.7	44	21.7
8	33	15.4	44	25.0	44	25.0	35	12.8	43	23.5	44	23.5
12	35	16.3	44	28.1	46	28.1	38	14.7	50	29.0	51	29.0

implies. In contrast, some of the unstructured subdomains contain two different materials, and condition number estimates continue to grow with increasing values of σ .

7.2. Three Dimensions. The numerical examples in this section mirror their 2D counterparts of the previous section. Because of significant computational requirements in 3D, attention is restricted to cases in which the ratio H/h is no larger than 12. Indeed, the local subproblems for the examples of this section were solved iteratively to machine precision for $H/h = 12$. The significant computational requirements of direct solvers in 3D highlights the need for algorithms which use inexact solutions of the local subdomains problems and quite possibly the global coarse problem as well. Such inexact methods will be the topic of a future investigation.

Results shown in Tables 7.6-7.9 and Figure 7.4 exhibit the same trends that were observed for the 2D examples. Compared with the 2D examples, we were not able to generate numerical results for as large of values of H/h . Nevertheless, results in Figure 7.4 are consistent with a condition number bound proportional to $1 + \log(H/h)$ for fixed values of H/δ , as was the case in 2D. As before, a much stronger dependence on the ratio H/δ is evident in Table 7.8 for almost incompressible materials.

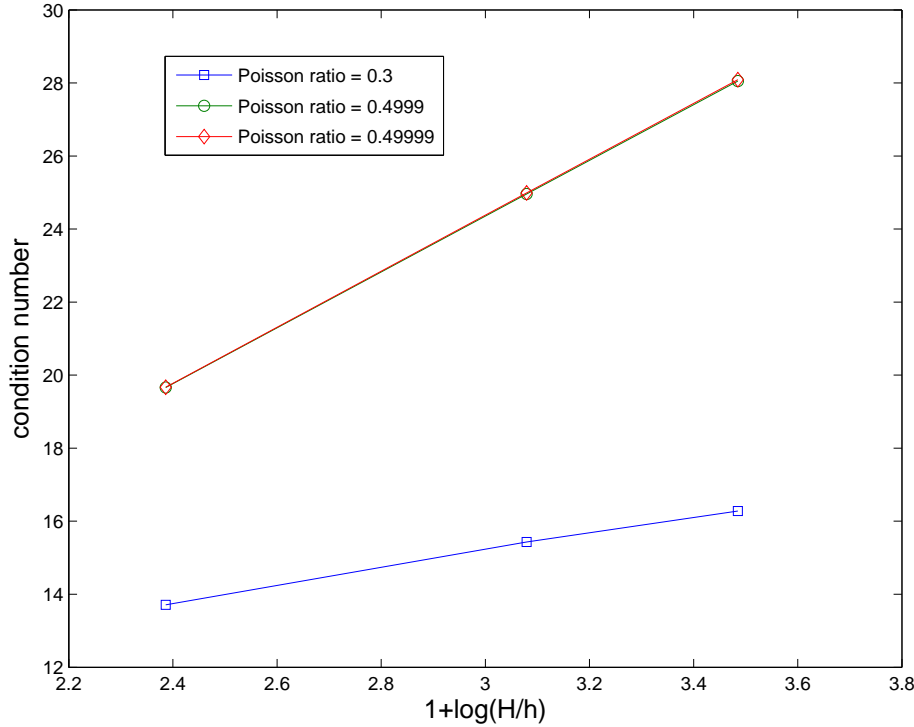


FIG. 7.4. Three dimensional results from Table 7.7.

TABLE 7.8

Three dimensional results for $N = 27$, $H/h = 12$, and increasing values of H/δ .

H/δ	structured decomposition				unstructured decomposition			
	$\nu = 0.3$		$\nu = 0.4999$		$\nu = 0.3$		$\nu = 0.4999$	
	iter	cond	iter	cond	iter	cond	iter	cond
4	35	16.3	44	28.1	35	12.9	43	21.7
6	38	20.8	51	34.8	41	16.4	51	31.1
12	51	30.7	86	123	47	21.5	74	71.2

TABLE 7.9

Three dimensional results for a problem with discontinuous material properties. In a centered cube region of dimension $1/3$, the elastic modulus equals σ and the Poisson ratio is 0.3 . For the remainder of the region, the elastic modulus is unity and the Poisson ratio is 0.49999 . Fixed values of $N = 27$, $H/h = 8$, and $H/\delta = 4$ are used.

σ	structured decomposition		unstructured decomposition	
	iter	cond	iter	cond
10^{-4}	44	22.0	45	21.3
10^2	43	22.0	44	21.3
1	45	23.8	45	22.6
10^2	47	27.5	63	55.7
10^4	46	27.7	83	201

REFERENCES

- [1] Gabriel Acosta, Ricardo G. Durán, and María A. Muschietti. Solutions of the divergence operator on John domains. *Adv. Math.*, 206(2):373–401, 2006.
- [2] Owe Axelsson. Preconditioning of indefinite problems by regularization. *SIAM J. Numer. Anal.*, 16(1):58–69, 1979.
- [3] Michele Benzi and Maxim A. Olshanskii. An augmented Lagrangian-based approach to the Oseen problem. *SIAM J. Sci. Comput.*, 28(6):2095–2113, 2006.
- [4] Manoj Bhardwaj, Garth Reese, Brian Driessen, Kenneth Alvin, and David Day. Salinas - an implicit finite element structural dynamics code developed for massively parallel platforms. In *41st AIAA/ASME/ASCE/AHS/ASC SDM April 3-6, 2000/Atlanta, GA*, AIAA 2000-1651.
- [5] Bogdan Bojarski. Remarks on Sobolev imbedding inequalities. In *Complex analysis, Joensuu 1987*, volume 1351 of *Lecture Notes in Math.*, pages 52–68. Springer, Berlin, 1988.
- [6] James H. Bramble. A proof of the inf-sup condition for the Stokes equations on Lipschitz domains. *Math. Models Methods Appl. Sci.*, 13(3):361–371, 2003.
- [7] Susanne C. Brenner and Ridgway Scott. *The Mathematical Theory of Finite Element Methods*. Springer-Verlag, Berlin, Heidelberg, New York, 2002. Second edition.
- [8] Franco Brezzi and Michel Fortin. *Mixed and Hybrid Finite Element Methods*. Springer-Verlag, 1991.
- [9] S. Buckley and P. Koskela. Sobolev-Poincaré implies John. *Math. Res. Lett.*, 2(5):577–593, 1995.
- [10] Mario A. Casarin. *Schwarz Preconditioners for Spectral and Mortar Finite Element Methods with Applications to Incompressible Fluids*. PhD thesis, Dept. of Mathematics, Courant Institute of Mathematical Sciences, New York University, March 1996. Tech. Rep. 717, Department of Computer Science, Courant Institute.
- [11] Arie C. de Niet and Fred W. Wubs. Two preconditioners for saddle point problems in fluid flows. *Int. J. Numer. Meth. Fluids*, 54:355–377, 2007.
- [12] Manfred Dobrowolski. On the LBB constant on stretched domains. *Math. Nachr.*, 254–255:64–67, 2003.
- [13] Clark R. Dohrmann. Preconditioning of saddle point systems by substructuring and a penalty approach. In David E. Keyes and Olof B. Widlund, editors, *Domain Decomposition Methods in Sciences and Engineering XVI*, number 55 in *Lecture Notes in Computational Science and Engineering*, pages 53–64. Springer-Verlag, 2006. Proceedings of the 16th International Conference on Domain Decomposition Methods, held in New York City, January 11–15, 2005.
- [14] Clark R. Dohrmann, Axel Klawonn, and Olof B. Widlund. A family of energy minimizing coarse spaces for overlapping Schwarz preconditioners. In Ulrich Langer, Marco Discacciati, David Keyes, Olof Widlund, and Walter Zulehner, editors, *Proceedings of the 17th International Conference on Domain Decomposition Methods in Science and Engineering, held in Strobl, Austria, July 3-7, 2006*, number 60 in *Springer-Verlag, Lecture Notes in Computational Science and Engineering*, pages 247–254, 2007.
- [15] Clark R. Dohrmann, Axel Klawonn, and Olof B. Widlund. Domain decomposition for less regular subdomains: Overlapping Schwarz in two dimensions. *SIAM J. Numer. Anal.*, 46(4):2153–2168, 2008.
- [16] Clark R. Dohrmann and Richard B. Lehoucq. A primal-based penalty preconditioner for elliptic saddle point systems. *SIAM J. Numer. Anal.*, 44(1):270–282, 2006.
- [17] Maksymilian Dryja, Barry F. Smith, and Olof B. Widlund. Schwarz analysis of iterative substructuring algorithms for elliptic problems in three dimensions. *SIAM J. Numer. Anal.*, 31(6):1662–1694, 1994.
- [18] Ricardo G. Durán and María A. Muschietti. The Korn inequality for Jones domains. *Electron. J. Differential Equations*, 2004(127):1–10, 2004.
- [19] Paulo Goldfeld, Luca F. Pavarino, and Olof B. Widlund. Balancing Neumann-Neumann preconditioners for mixed approximations of heterogeneous problems in linear elasticity. *Numer. Math.*, 95(2):283–324, 2003.
- [20] Peter W. Jones. Quasiconformal mappings and extendability of functions in Sobolev space. *Acta Math.*, 147(1-2):71–88, 1981.
- [21] George Karypis and Vipin Kumar. *METIS Version 4.0*. University of Minnesota, Department of Computer Science, Minneapolis, MN, 1998.
- [22] Axel Klawonn and Luca F. Pavarino. Overlapping Schwarz methods for mixed linear elasticity and Stokes problems. *Comput. Methods Appl. Mech. Engrg.*, 165:233–245, 1998.
- [23] Axel Klawonn and Luca F. Pavarino. A comparison of overlapping Schwarz methods and block

- preconditioners for saddle point problems. *Numer. Lin. Alg. Appl.*, 7:1–25, 2000.
- [24] Axel Klawonn and Oliver Rheinbach. Robust FETI-DP methods for heterogeneous three dimensional linear elasticity problems. *Comput. Methods Appl. Mech. Engrg.*, 196(8):1400–1414, 2007.
- [25] Axel Klawonn, Oliver Rheinbach, and Olof B. Widlund. An analysis of a FETI–DP algorithm on irregular subdomains in the plane. Technical Report TR2007-889, Department of Computer Science, Courant Institute of Mathematical Sciences, New York University, April 2007. URL: <http://cs.nyu.edu/csweb/Research/TechReports/TR2007-889/TR2007-889.pdf>. To appear in *SIAM J. Numer. Anal.*
- [26] Axel Klawonn and Olof B. Widlund. Dual-Primal FETI methods for linear elasticity. *Comm. Pure Appl. Math.*, 59(11):1523–1572, November 2006.
- [27] Jing Li. A dual-primal FETI method for incompressible Stokes equations. *Numer. Math.*, 102:257–275, 2005.
- [28] Jing Li and Olof B. Widlund. BDDC algorithms for incompressible Stokes equations. *SIAM J. Numer. Anal.*, 44(6):2432–2455, 2006.
- [29] Jan Mandel. Iterative solvers by substructuring for the p-version finite element method. *Comput. Methods Appl. Mech. Engrg.*, 80:117–128, 1990.
- [30] Jindřich Nečas. *Les méthodes directes en théorie des équations elliptiques*. Academia, Prague, 1967.
- [31] Barry F. Smith, Petter Bjørstad, and William Gropp. *Domain Decomposition: Parallel Multilevel Methods for Elliptic Partial Differential Equations*. Cambridge University Press, New York, 1996.
- [32] Rolf Stenberg. A technique for analysing finite element methods for viscous incompressible flow. *Internat. Inter. J. Numer. Methods Fluids*, 11:935–948, 1990.
- [33] Andrea Toselli and Olof Widlund. *Domain Decomposition Methods - Algorithms and Theory*, volume 34 of *Springer Series in Computational Mathematics*. Springer-Verlag, Berlin Heidelberg New York, 2005.